STEM CELLS AND DEVELOPMENT
Volume 24, Number 11, 2015

DOI: 10.1089/scd.2014.0402

Catalase Inhibits Ionizing Radiation-Induced Apoptosis in Hematopoietic Stem and Progenitor Cells

Xia Xiao,[1,2] Hongmei Luo,[1,3] Kenneth N. Vanek,[4] Amanda C. LaRue,[1,5,6] Bradley A. Schulte,[1] and Gavin Y. Wang[1,6]

Hematologic toxicity is a major cause of mortality in radiation emergency scenarios and a primary side effect concern in patients undergoing chemo-radiotherapy. Therefore, there is a critical need for the development of novel and more effective approaches to manage this side effect. Catalase is a potent antioxidant enzyme that coverts hydrogen peroxide into hydrogen and water. In this study, we evaluated the efficacy of catalase as a protectant against ionizing radiation (IR)-induced toxicity in hematopoietic stem and progenitor cells (HSPCs). The results revealed that catalase treatment markedly inhibits IR-induced apoptosis in murine hematopoietic stem cells and hematopoietic progenitor cells. Subsequent colony-forming cell and cobble-stone area-forming cell assays showed that catalase-treated HSPCs can not only survive irradiation-induced apoptosis but also have higher clonogenic capacity, compared with vehicle-treated cells. Moreover, transplantation of catalase-treated irradiated HSPCs results in high levels of multi-lineage and long-term engraftments, whereas vehicle-treated irradiated HSPCs exhibit very limited hematopoiesis reconstituting capacity. Mechanistically, catalase treatment attenuates IR-induced DNA double-strand breaks and inhibits reactive oxygen species. Unexpectedly, we found that the radioprotective effect of catalase is associated with activation of the signal transducer and activator of transcription 3 (STAT3) signaling pathway and pharmacological inhibition of STAT3 abolishes the protective activity of catalase, suggesting that catalase may protect HSPCs against IR-induced toxicity via promoting STAT3 activation. Collectively, these results demonstrate a previously unrecognized mechanism by which catalase inhibits IR-induced DNA damage and apoptosis in HSPCs.

Introduction

Myelosuppression is the most common dose-limiting side effect of conventional cancer therapy using ionizing radiation (IR) and/or certain chemotherapeutic agents [1–3]. In the event of an acute radiation disaster caused by a possible nuclear terrorism attack, a nuclear power plant accident, or nuclear warfare, a large population of civilians and particularly the first responders are at high risk of IR exposure. Bone marrow (BM) hematopoietic cells are highly sensitive to chemotherapy and radiation-induced toxicity. Even a moderate dose (eg, 3 Gy) of IR exposure can cause acute myelosuppression characterized by neutropenia, lymphocytopenia, and thrombocytopenia. It is well documented that hematopoietic acute radiation syndrome increases the risk of infection, bleeding, and even death [4–9]. Moreover, during the course of radiation and chemotherapy, therapy-induced myelosuppression may cause high mortality and morbidity and worsen the outcome of cancer treatment [2,4–8]. Studies from ours and other laboratories have demonstrated that radiation-caused acute myelosuppression is largely attributable to the induction of apoptosis in hematopoietic stem and progenitor cells (HSPCs) [3,6]. Therefore, there is a critical need for the development of new and more effective radioprotective agents that can be used to protect IR-induced apoptosis in BM HSPCs.

We and others have shown that the generation of reactive oxygen species (ROS) plays a critical role in IR-induced normal tissue toxicity, including BM radiation injury [10–13]. IR induces ROS production in cells as a consequence of radiolysis of water, and these ROS include superoxide, hydrogen peroxide (H_2O_2), hydroxyl radicals, and so on. If the

[1]Department of Pathology and Laboratory Medicine, Medical University of South Carolina, Charleston, South Carolina.
[2]Department of Hematology, Tianjin First Center Hospital, Tianjin, People's Republic of China.
[3]Department of Histology and Embryology, University of South China, Hengyang City, Hunan Province, People's Republic of China.
[4]Department of Radiation Oncology, Medical University of South Carolina, Charleston, South Carolina.
[5]Research Services, Ralph H. Johnson VAMC, Charleston, South Carolina.
[6]Cancer Genes and Molecular Regulation Program of the Hollings Cancer Center, Medical University of South Carolina, Charleston, South Carolina.

accumulation of ROS exceeds the capacity of the antioxidant system, oxidative stress can cause DNA damage, leading to apoptosis and/or cellular senescence [3,6,10,14–16]. Given the significant involvement of ROS in IR-induced cell killing and normal tissue damage, it has been proposed that the use of certain antioxidants might be helpful for the prevention of radiation toxicity [10,12,17,18].

Catalase (CAT) is an endogenous antioxidant enzyme found in almost all living organisms, which functions as a potent ROS scavenger via catalyzing the conversion of H_2O_2 into water and oxygen. It has been shown that ectopic overexpression of CAT can protect a variety of tissues against oxidative stress-induced damage in animal models [19–21]. Furthermore, there is evidence indicating that CAT treatment may preserve hematopoietic stem cell (HSC) self-renewal in long-term BM cultures [22]. However, the potential of exogenous CAT to protect against IR-induced HSPC apoptosis remains to be determined. In this study, we have found that CAT treatment in vitro protects against radiation-induced DNA damage and apoptosis via promoting STAT3 activation in HSPCs. Importantly, data from competitive repopulation assays (CRA) have shown that CAT-rescued irradiated HSPCs retain the ability of self-renewal and can reconstitute the hematopoietic system in lethally irradiated recipient mice. These results demonstrate, for the first time, the usefulness of exogenous CAT for ameliorating radiation-induced hematologic toxicity.

Materials and Methods

Reagents

Phycoerythrin (PE)-conjugated anti-Sca-1 (Clone E13-161.7, rat IgG2a); APC-conjugated anti-c-kit (Clone 2B8, rat IgG2b); PE-conjugated anti-CD45R/B220 (Clone RA3-6B2, rat IgG2a); anti-Gr-1 (Clone RB6-8C5, rat IgG2b); anti-Mac-1 (Clone M1/70, rat IgG2b); anti-Ter-119 (Clone Ter-119, rat IgG2b); and purified rat anti-CD 16/CD32 (Clone 2.4G2, Fcγ receptor blocker, rat IgG2b) were purchased from BD Pharmingen. Monoclonal antibodies against cleaved caspase-3, survivin, p-chk1, chk1, p-chk2, chk2, p-SATT3, STAT3, and ATM were purchased from Cell Signaling. Mouse Hematopoietic Progenitor (Stem) Cell Enrichment Set-DM was purchased from BD Biosciences. Recombinant mouse thrombopoietin (Tpo) was purchased from R&D Systems. Catalase was obtained from Sigma. The mouse anti-phospho-histone H2AX (γH2AX) monoclonal antibody was purchased from Millipore. The Alexa fluor-555-conjugated goat anti-rabbit IgG antibody and 2′, 7′-dichlorodihydrofluorescein diacetate (DCF-DA) were purchased from Invitrogen.

Mice

Male C57BL/6-Ly-5.2 (Ly5.2) and C57BL/6-Ly-5.1 (Ly5.1) mice were purchased from The Jackson Laboratories. Mice were housed four to five per cage at the Medical University of South Carolina (MUSC) AAALAC-certified animal facility. They received food and water ad libitum. All mice were used at approximately 8 to 12 weeks of age. The Institutional Animal Care and Use Committee of MUSC approved all experimental procedures used in this study.

Isolation of BM mononuclear cells and lineage-negative HSPCs

BM mononuclear cells (BM-MNCs) were isolated as previously described [3,6]. Lineage-negative HSPCs (Lin^- HSPCs) were enriched and purified using a mouse Progenitor and Stem Cell Enrichment Kit (BD Biosciences) according to the manufacturer's protocol. Briefly, mouse BM-MNCs were labeled with the biotinylated mouse lineage depletion cocktail containing monoclonal antibodies against mouse CD3e, CD11b, CD45R/B220, Gr-1, and Ter-119. Cells committed to the T- and B-lymphocytic, myeloid, and erythroid lineages were then depleted by MACS using the BD IMag™ streptavidin magnetic beads (BD Biosciences).

Flow cytometric apoptosis assay

Lin^- HSPCs were cultured in IMDM medium containing 10% FBS and 20 ng/mL mouse recombinant Tpo. Cells were preincubated with 100 U/mL CAT or an equal volume of PBS as a vehicle control for 30 min before IR exposure (2 Gy). At 24 h after irradiation, cells were collected and stained with PE-conjugated anti-Sca1 and APC-conjugated anti-c-kit antibodies. Cells were then stained with FITC-Annexin V using an apoptosis assay kit (BD Biosciences) according to the manufacturer's protocol. Apoptotic cells were determined by flow cytometric analysis on an FACS Caliber (Becton Dickinson), and the data were analyzed using the CellQuest software as previously reported [3].

Colony-forming cell and cobblestone area-forming cell assays

Colony-forming cell (CFC) assays were performed by culturing the irradiated and control HSPCs in MethoCult GF M3434 methylcellulose medium (Stem Cell Technologies) according to the manufacturer's protocol. Colonies of colony-forming unit-granulocyte macrophage (CFU-GM) and burst-forming unit-erythroid (BFU-E) were scored on day 7, while colonies of CFU-granulocyte, -erythrocyte, -monocyte, and -megakaryocyte (CFU-GEMM) were enumerated on day 12 after incubation. Cobblestone area-forming cell (CAFC) assays were conducted to evaluate HSC activity in vitro as previously reported [3,6]. Day-14 and -35 CAFC frequencies were determined to measure the clonogenic function of hematopoietic progenitor cells (HPCs) and HSCs, respectively, as previously described [6,23].

Competitive repopulating assay

Lin^- HSPCs were isolated from Ly5.1 (CD45.1) mice and incubated with 100 U/mL CAT or PBS as a vehicle control for 30 min before IR exposure (2 Gy). The irradiated cells were then cultured at 50,000 cells/well in IMDM medium containing 10% FBS and 20 ng/mL mouse recombinant Tpo in a 12-well plate. Twenty-four hours after IR, cells (50,000 initial HSPCs and their progeny per well) were harvested from cultures and mixed with 2×10^5 BM-MNCs isolated from Ly5.2 (CD45.2) mice as competitor cells. The mixed cells were then transplanted into lethally irradiated (9.5 Gy TBI) Ly5.2 mice by tail-vein injection. Peripheral-blood samples were obtained from the retro-orbital plexus using heparin-coated micropipettes (Drummond Scientific) at 8

and 16 weeks after transplantation. After red blood cells had been removed by lyses with 0.15 M NH_4Cl, samples were stained with FITC-conjugated anti-CD45.1 and PE-conjugated anti-CD45.2 to analyze donor-derived cells on an FACS Caliber (Becton Dickinson). Donor-derived engraftment ($CD45.1^+$ cells) in T-, B-lymphocytic, and myeloid lineages was evaluated by staining the cells with PE-conjugated anti-Thy-1.2, B220, and Gr-1/Mac-1 monoclonal antibodies, respectively.

Secondary transplantation

BM-MNCs were isolated from the primary recipients at 20 weeks after BM transplantation (BMT) and were used for the secondary transplantation. Because the frequency of HSCs in BM-MNCs is much lower than that in Lin^- cells, 5×10^5 BM-MNCs (rather than 5×10^4 Lin^- cells) were transplanted into each lethally irradiated (9.5 Gy TBI) recipient (CD 45.2) mouse. Eight weeks after secondary transplantation, donor cell engraftment ($CD45.1^+$ cells) was determined by flow cytometric analysis as described earlier.

Flow cytometric analysis of ROS

Intracellular ROS were measured by flow cytometric analysis as previously reported [10,12]. Briefly, Lin^- HSPCs were loaded with 5 μM of DCF-DA and incubated at 37°C for 30 min. The levels of ROS in HSPCs were analyzed by measuring the mean fluorescence intensity of DCF-DA staining using an FACSCalibur flow cytometer.

Immunofluorescent microscopic analysis of γH2AX foci

Phosphorylated H2AX (γH2AX) foci assays were performed to determine DNA double-strand breaks (DSBs) in HSPCs after CAT and/or IR treatments using immunofluorescent microscopic analysis as previously described [10,24]. Briefly, HSPCs were harvested from cultures and cytospun onto slides. Cells were fixed in 4% paraformaldehyde solution for 10 min and permeabilized with 0.2% Triton X-100. After incubation with anti-γH2AX (1:500) for 2 h at room temperature, γH2AX foci were visualized using Alexa Fluor 555-conjugated anti-mouse IgG antibody. Nuclei were counterstained with DAPI. The images were captured and processed using a Zeiss Axio Observer Z1 microscope.

Comet assay

A neutral comet assay was employed to determine DNA DSBs in HSPCs by using a Comet Assay® Kit (Trevigen) as previously described [25]. Briefly, cells were mixed with Comet Assay™ low-melting agarose at a ratio of 1: 10 (v/v) and spread evenly on slides. The cells were treated with CometAssay lysis solution at 4°C for 1 h, submerged in cold neutral electrophoresis buffer, and subjected to electrophoresis at 21V for 30 min. The cells were stained with SYBR® Green I and viewed using a Zeiss Axio Observer Z1 microscope. The images were captured and processed using the AxioVision (4.7.1.0) software (Carl Zeiss). The percentage of DNA tail moment was evaluated using the TriTek Comet Score™ software (Version 1.5.2.6; TriTek Corporation).

Western blotting analysis

Protein samples were extracted using cell lysis buffer (Cell Signaling) supplemented with a cocktail of proteinase inhibitors (Sigma). The protein concentrations were quantified using the Bio-Rad Dc protein assay kit (Bio-Rad Laboratories). Western blotting analysis was performed as previously described [24]. Briefly, 50 mg of protein samples were resolved on 10% Mini-Protean TGX gels (Bio-Rad) and transferred onto 0.2 μM PVDF membrane (Millipore). Blots were blocked with 5% nonfat milk for 1–2 h at room temperature, then probed with primary antibodies, and incubated at 4°C overnight. After extensive washing with TBS-T, blots were incubated with appropriate HRP-conjugated secondary antibody for 1.5 h at room temperature. Protein bands were detected using an ECL Plus Western Blotting Detection System (GE Healthcare Life Science).

Statistical analysis

Comparisons between two groups were carried out using Student's *t*-test. Multiple-group comparisons were performed using analysis of variance. Differences were considered statistically significant at $P<0.05$. All analyses were carried out with the GraphPad Prism program (GraphPad Software, Inc.).

Results

CAT inhibits IR-induced apoptosis in HSCs and HPCs

Our previous studies have shown that radiation-induced acute hematopoietic toxicity is, at least in part, attributable to the induction of apoptosis in HSPCs [3,6]. Given the important role of ROS production in mediating IR-induced normal tissue injury [10–16], we hypothesized that inhibition of ROS by the addition of exogenous CAT to cultures in vitro may protect HSPCs against IR-induced apoptosis. To test this hypothesis, we pretreated Lin^- HSPCs with exogenous CAT before IR exposure to determine the effects of CAT treatment on IR-induced apoptosis in HSPCs. The data show that preincubation with CAT significantly reduces the number of cells undergoing IR-induced apoptosis in both Lin^- $Sca1^+$ $c\text{-}Kit^+$ (LSK^+ cells or HSCs) and Lin^- $Sca1^+$ $c\text{-}Kit^-$ (LSK^- cells, or HPCs) subpopulations (Fig. 1A–C). These results indicate that exogenous CAT treatment inhibits IR-induced apoptosis in both HSCs and HPCs. In addition, the ability of CAT to inhibit IR-induced apoptosis in irradiated HSPCs was further confirmed by cleaved caspase-3 assays (Fig. 1D, E).

CAT treatment protects the clonogenic capacity of irradiated HSPCs

Next, we asked whether the CAT-rescued HSPCs have the potential to generate hematopoietic colonies in cultures. To address this question, CFU assays were performed to determine the colony-forming activity of HPCs. As shown in Fig. 2A–**C**, CAT-treated irradiated HSPCs produce a greater number of CFU-GM, BFU-E, and CFU-GEMM than do PBS-treated irradiated cells. These data suggest that CAT treatment protects the clonogenic function of HSPCs and

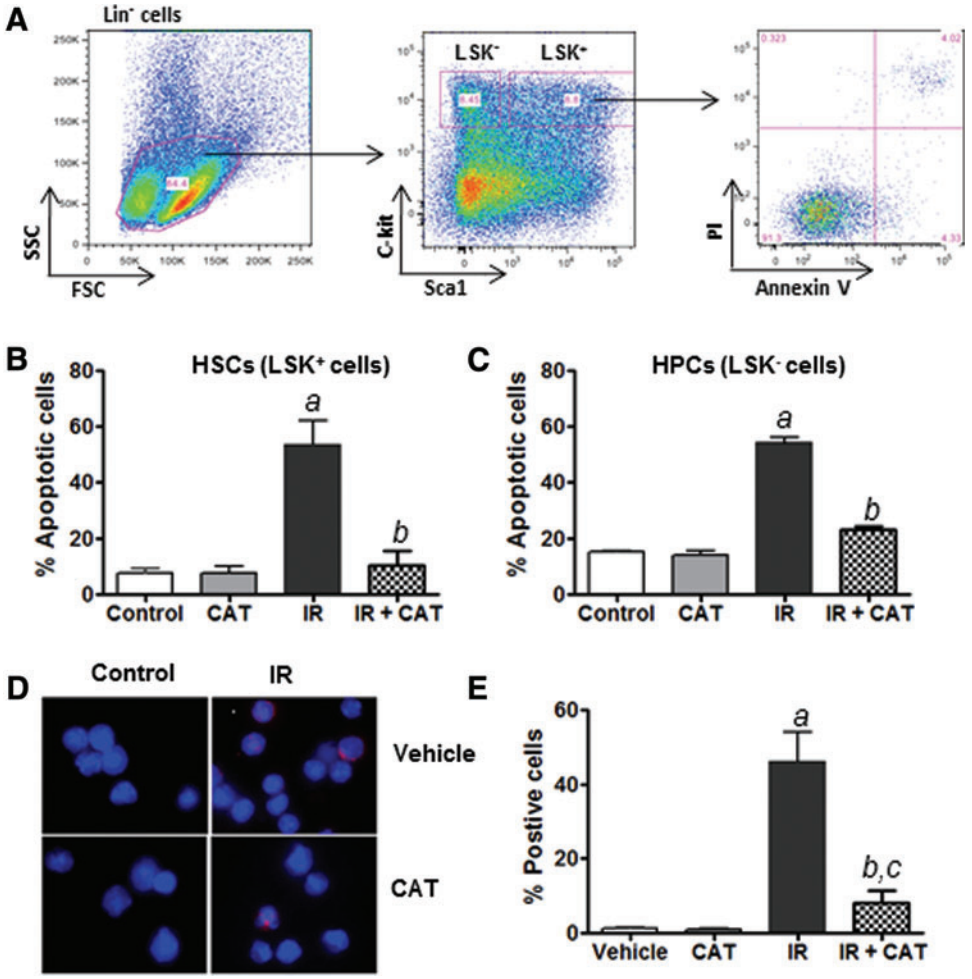

FIG. 1. Catalase (CAT) inhibits IR-induced apoptosis in hematopoietic stem cells (HSCs) and hematopoietic progenitor cells (HPCs). **(A)** Schematic illustration of apoptosis analysis in Lin^- $Sca1^+$ c-Kit^+ (LSK^+) HSCs and Lin^- $Sca1^+$ c-Kit^- (LSK^-) HPCs. **(B)** The percentage of apoptotic cells in HSCs after IR and CAT treatment is presented as mean ± SEM of three independent experiments. **(C)** The percentage of apoptotic cells in HPCs after IR and CAT treatment is presented as mean ± SEM of three independent experiments. **(D)** Lin^- HSPCs were pretreated with CAT (100 U/mL) or PBS as vehicle control for 30 min before IR. Cleaved caspase-3 immunostaining was performed at 16 h after IR. Representative photomicrographs of activated caspase-3 immunofluorescent staining (*red*) and nucleic counterstaining with DAPI (*blue*) are shown. **(E)** The percentage of cells positively stained for cleaved caspase-3 in different groups of HSPCs is presented as mean ± SEM of three independent assays. $^aP < 0.001$ versus PBS vehicle control; $^bP < 0.01$ versus IR; $^cP < 0.05$ versus PBS vehicle control. Color images available online at www.liebertpub.com/scd

that CAT-rescued HSPCs retain the ability to differentiate into multi-lineage hematopoietic colonies.

To further determine whether the CAT-rescued HSPCs retain HSC functional activity, we employed CAFC assays to evaluate the clonogenic capacity of HSCs in vitro. Both day-14 and -35 CAFCs generated from CAT-treated HPSCs were markedly higher relative to those generated from PBS-treated cells (Fig. 2D, E). Given that the day-35 CAFC is a surrogate of HSC measurement in vitro [6,23], these results suggest that CAT treatment may protect the clonogenic ability of irradiated HSCs.

CAT treatment retains the self-renewal potential of irradiated HSPCs in vivo

BMT is the gold standard assay to evaluate the self-renewal potential of HSCs. Therefore, we performed CRA to further examine the self-renewal function of CAT-rescued irradiated HSPCs in vivo. At 8 and 16 weeks after BMT, peripheral blood cells from the recipient mice were analyzed for donor cell-derived engraftment. The results indicate that CAT-treated HSPCs exhibit significantly higher donor cell-derived engraftment than do cells treated with PBS as vehicle control (Fig. 3A, B). Moreover, flow cytometric assays show that CAT-treated irradiated HSPCs give rise to higher levels of myeloid, B- and T-lymphocytic lineage engraftments in recipient mice as compared with PBS-treated irradiated donor cells (Fig. 3C).

Secondary transplantation analyses reveal that CAT-treated cells can repopulate all lineages of the blood cells, while PBS-treated HSPCs exhibit only very limited ability to generate donor-derived hematopoietic cells in recipient mice (Fig. 3D, E). When examining donor-derived bone marrow HSCs (LSK^+ Cells) reconstitution, we found that

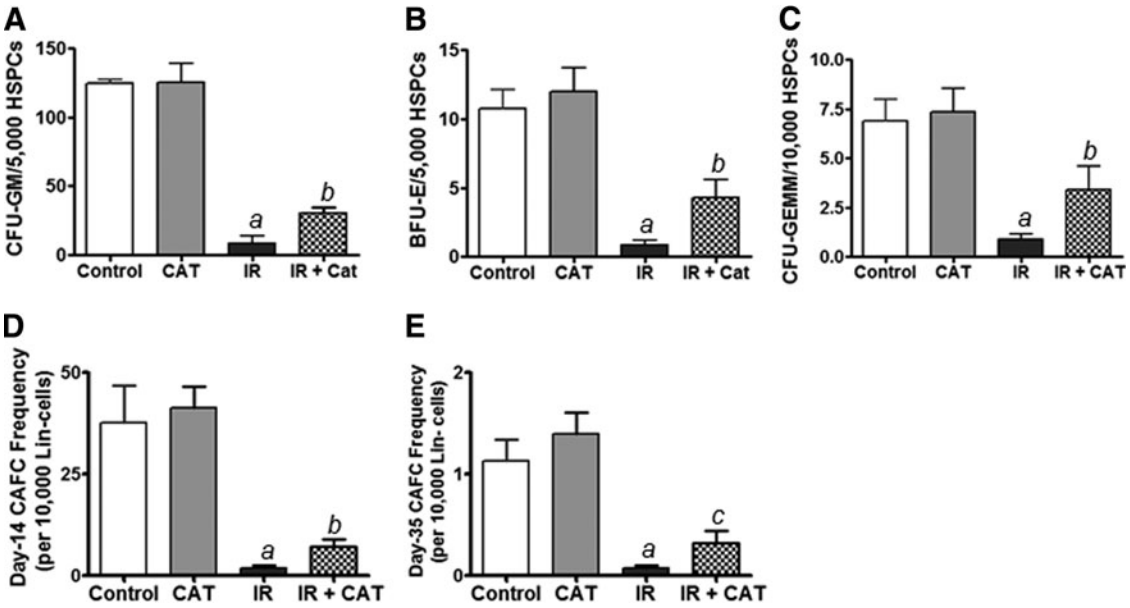

FIG. 2. CAT treatment protects the clonogenic function of irradiated HSPCs. **(A–C)** Colony-forming cell (CFC) assays were performed to determine the clonogenic capacity of HPCs to generate CFU-E, BFU-E, and CFU-GEMM as previously reported [3,6]. **(D, E)** CAFC assays were employed to examine the clonogenic functions of HPCs (day-14 CAFCs) and HSCs (day-35 CAFCs), respectively, as previously described [6,23]. Data are presented as mean ± SEM of three independent experiments. $^{a}P < 0.01$ versus PBS vehicle control; $^{b}P < 0.05$ versus IR; $^{c}P < 0.01$ versus IR.

CAT-treated irradiated HSPCs contribute to 16.3% of donor-derived HSCs compared with only 2.6% of donor-derived HSCs produced by PBS-treated irradiated HSPCs, indicating a 6.3-fold increase in HSC reconstruction by CAT treatment (Fig. 3F). Together, these findings demonstrate that CAT-rescued irradiated HSPCs retain the self-renewal ability and, thus, can reconstitute long-term and multilineage hematopoiesis in lethally irradiated recipient mice.

CAT inhibits IR-induced ROS production in HSPCs

We and others have shown that the production of ROS plays a critical role in IR-induced toxicity [10–16], suggesting that CAT may protect HSPCs against radiation toxicity via inhibiting IR-induced ROS production. To test this hypothesis, we investigated the levels of ROS in irradiated HSPCs with or without CAT treatment. DCF-DA staining and flow cytometric analyses reveal that IR increases ROS levels in both HSCs and HPCs (Fig. 4). Furthermore, CAT treatment significantly reduces the levels of ROS in irradiated HSCs and HPCs (Fig. 4B, C). These results strongly support the hypothesis that CAT may protect against radiation-induced apoptosis in HSPCs via inhibiting the production of ROS caused by IR.

CAT treatment attenuates IR-induced DNA damage in HSPCs

It has been shown that IR-induced DNA damage significantly contributes to radiation toxicity [10,15,18]. However, it has not been determined whether CAT treatment has any effects on IR-induced DNA damage in HSPCs. To address this important issue, we performed γH2AX foci assays to assess the effects of CAT treatment on IR-induced DNA double-strand breaks (DSBs) in irradiated HSPCs. As shown in Fig. 5A–C, IR-induced γH2AX foci were substantially reduced by CAT treatment in irradiated HSPCs, compared with cells treated with PBS as a vehicle control. CAT treatment significantly decreased IR-induced γH2AX foci at 60 min after irradiation (Fig. 5B), demonstrating that CAT prevents IR-induced DNA damage in HSPCs. However, the reduction of γH2AX foci by CAT at 24 h after irradiation was not as pronounced as it did at 60 min post IR (Fig. 5B, C), suggesting that CAT may protect HSPCs against irradiation mainly through inhibition of IR-induced DNA DSBs while having only a limited effect on promoting DNA repair.

Consistent with the earlier findings, comet assay data further confirmed that CAT treatment inhibits IR-induced DNA DSBs in HSPCs (Fig. 5D, E). Together with the observations that CAT treatment diminishes IR-induced production of ROS (Fig. 4), these data suggest that CAT may protect HSPCs against IR-induced apoptosis via inhibiting ROS-mediated DNA damage.

CAT protects HSPCs against IR-induced apoptosis via promoting STAT3 activation

STAT3 has been shown to play an important role in HSPC survival, self-renewal, proliferation, and differentiation [26–29]. To better understand the mechanisms by which CAT protects HSPCs against IR-induced cell death, we investigated the effects of CAT treatment on STAT3 signaling in HSPCs. Surprisingly, we found that CAT treatment markedly increases the phosphorylation of STAT3, but it shows no significant effects on total STAT3 protein levels (Fig. 6A). These results demonstrate for the first time that CAT treatment somehow can promote STAT3 activation in

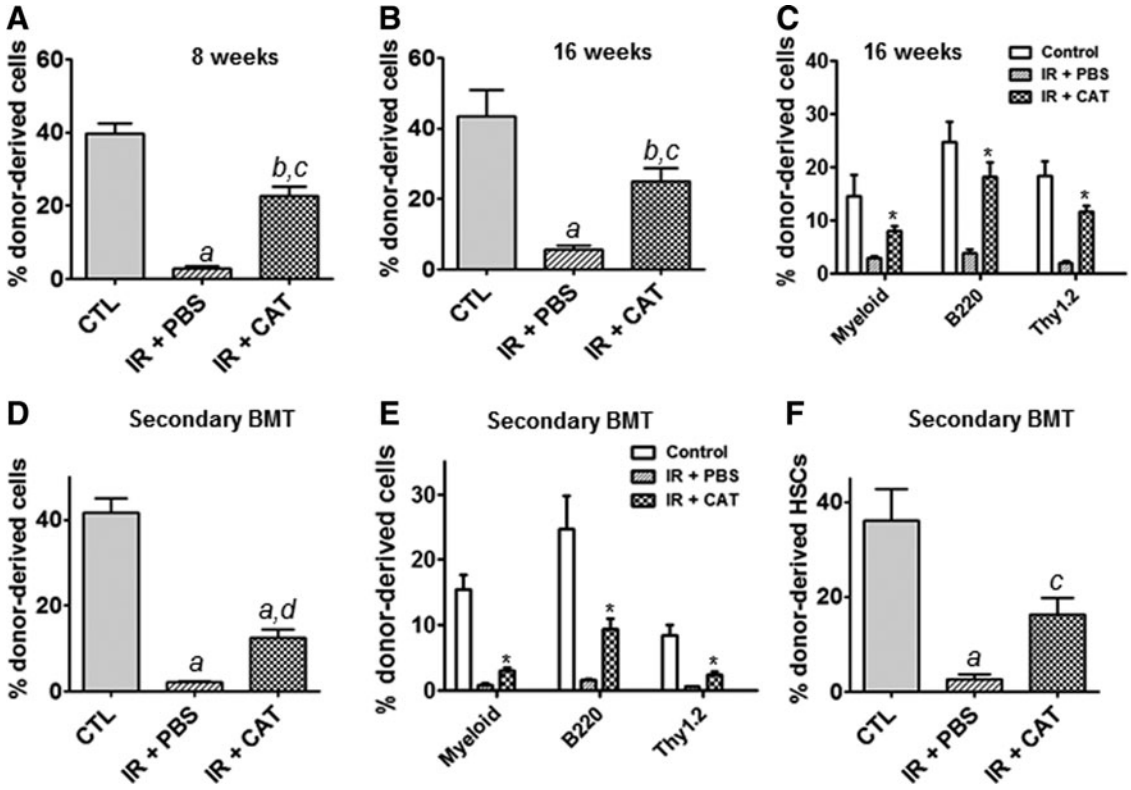

FIG. 3. Transplantation of CAT-rescued irradiated HSPCs produces long-term engraftment in recipient mice. Competitive repopulation assays (CRA) were performed to determine the self-renewal and multi-lineage differentiation capacity of HSCs. **(A)** Short-term donor cell-derived engraftment in peripheral blood was determined at 8 weeks post transplantation using flow cytometric analyses. **(B)** Long-term donor cell-derived engraftment in peripheral blood was determined at 16 weeks after transplantation. **(C)** Shown is the percentage of donor cell-derived myeloid, B-, and T-lymphocytic lineage engraftment at 16 weeks post transplantation. Data are presented as mean ± SEM ($n = 10$ mice per group). **(D)** Donor cell-derived engraftment in peripheral blood was determined at 8 weeks after secondary bone marrow transplantation (BMT). **(E)** Shown is the percentage of donor cell-derived myeloid, B-, and T-lymphocytic lineage engraftment at 8 weeks after secondary BMT. Data are presented as mean ± SEM ($n = 5$ mice per group). **(F)** Donor cell-derived HSC (LSK^+ cell) reconstitutions in bone marrow of recipient mice were determined at 8 weeks after secondary transplantation. $^aP < 0.001$ versus Control (CTL); $^bP < 0.01$ versus CTL; $^cP < 0.01$ versus IR + PBS; $^dP < 0.05$ versus IR + PBS; $^*P < 0.001$ versus IR + PBS.

HSPCs. To determine whether CAT treatment also affects the activity of other cell survival signaling pathways in HSPCs, we examined the effects of CAT treatment on the phosphorylation of extracellular signal-regulated kinase (Erk). The data show that CAT treatment has no significant effect on the expression of phosphorylated Erk in HSPCs. These results suggest that CAT may selectively promote the activation of the STAT3 signaling pathway in HSPCs. In agreement with this suggestion, our subsequent studies further show that the expression of survivin, a down-stream target of STAT3, is significantly increased in irradiated HSPCs by CAT treatment (Fig. 6A).

Given the implications of the ATM-chk2 and ATR-chk1 pathways in modulating DNA damage response, we investigated whether CAT treatment affects the activation of these two signaling pathways in HSPCs. As shown in Fig. 6B, western blot analyses indicate that CAT treatment markedly enhances IR-induced increase in phosphorylated chk2 expression. However, no significant changes were observed in both phosphorylated chk1 and total chk1 expression. These results suggest that CAT treatment may also enhance the activation of the ATM-chk2 pathway and thus promote DNA damage response in HSPCs.

To verify the specificity of STAT3 activation by CAT, we preincubated HSPCs with an STAT3 specific small-molecule inhibitor, Stattic [30], and confirmed that Stattic (ST) treatment blocks CAT-mediated STAT3 activation in HSPCs (Fig. 6C). In addition, apoptosis assays demonstrate that inhibition of STAT3 activation by ST abolishes the protective effect of CAT in HSPCs (Fig. 6D, E). Together, these novel observations suggest that CAT may protect HSPCs against IR-induced apoptotic cell death via promoting the activation of the STAT3 signaling pathway.

Discussion

Bone marrow is one of the most radiation sensitive tissues; even a relatively low dose of radiation exposure may lead to significant BM injury that will place victims at a life-threatening risk of severe infections, hemorrhage, and even death [4–10]. Previous studies, including those from our laboratory, indicated that acute BM radiation injury is, at least in part, attributable to the induction of apoptosis in HSPCs [3,6,18], suggesting that inhibition of IR-induced apoptosis may be an effective approach to protecting BM radiation injury. CAT is an extremely potent antioxidant

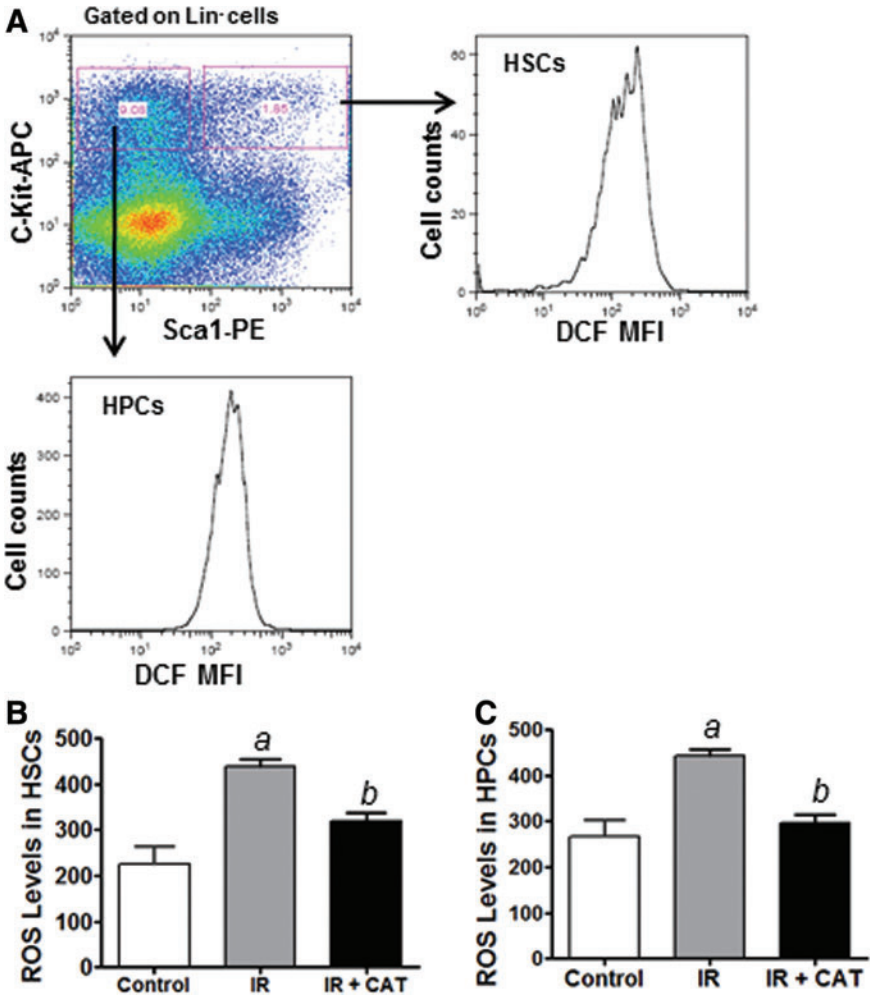

FIG. 4. CAT inhibits IR-induced reactive oxygen species (ROS) production in HSPCs. **(A)** Schematic illustration of ROS analysis in HSCs and HPCs using DCF staining along with flow cytometric analysis as previously reported [10]. **(B)** ROS levels in HSCs are presented as mean fluorescence intensity (MFI) of 2′, 7′-dichlorofluorescein (DCF) staining. **(C)** ROS levels in HPCs are presented as DCF MFI of three independent assays. $^{a}P<0.01$ versus control; $^{b}P<0.05$ versus IR. Color images available online at www.liebertpub.com/scd

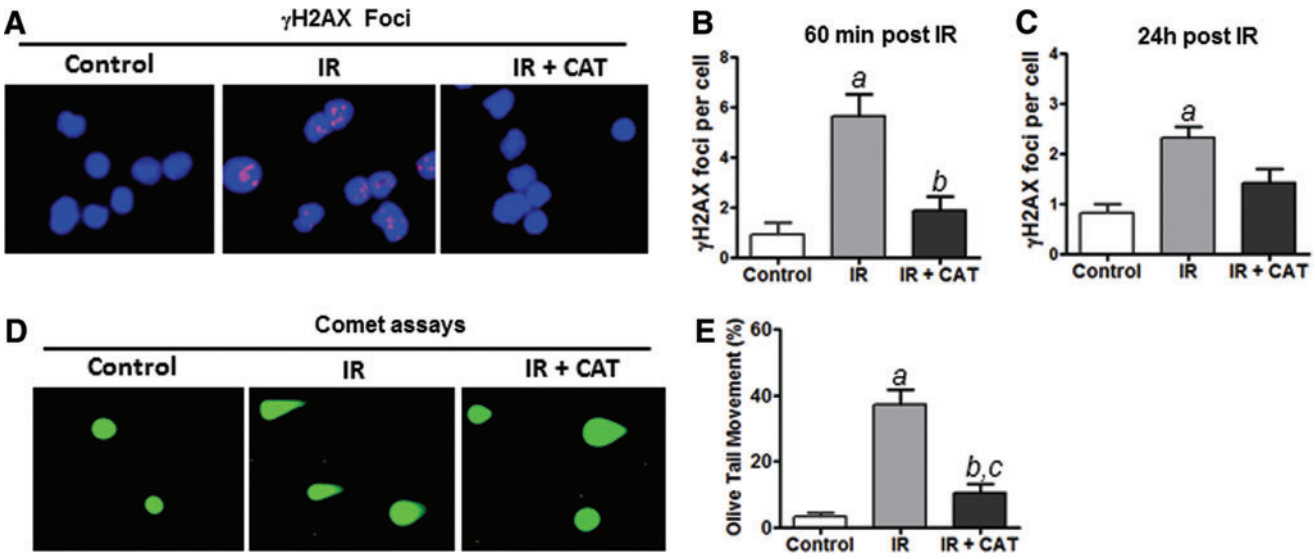

FIG. 5. CAT treatment attenuates IR-induced DNA damage in HSPCs. **(A)** Representative photomicrographs of γH2AX immunofluorescent staining (*red*) and nucleic counterstaining with DAPI (*blue*) are shown. **(B)** Numbers of γH2AX foci/cell at 60 min after IR are presented as mean ± SEM of three independent assays. **(C)** Numbers of γH2AX foci/cell at 24 h post IR are presented as mean ± SEM of three independent assays. **(D)** Representative photomicrographs of comet assays are shown. **(E)** The percentage of tail DNA movement in HSPCs with different treatments was quantified and graphed. Data are presented as mean ± SEM of three independent assays. $^{a}P<0.01$ versus control; $^{b}P<0.05$ versus IR; $^{c}P<0.05$ versus control. Color images available online at www.liebertpub.com/scd

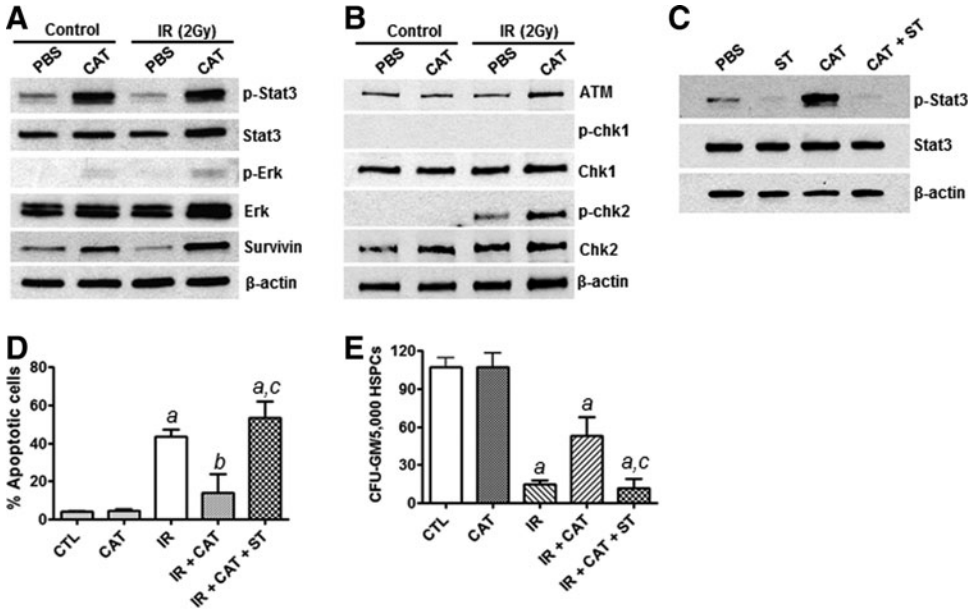

FIG. 6. CAT treatment promotes STAT3 activation in HSPCs. **(A)** Western blots were performed to determine the expression levels of phosphorylated Stat3 (p-Stat3) and phosphorylated Erk (p-Erk) as well as total Stat3, Erk, and survivin proteins in HSPCs. β-actin was probed as a loading control. **(B)** The activation of the ATM-chk2 and ATR-chk1 pathways was determined by western blots using phosphorylated chk1 (p-chk1) and phosphorylated chk2 (p-chk2) specific antibodies. **(C)** Western blot analyses were performed to examine the effects of Stattic (ST) on CAT-mediated Stat3 activation in HSPCs. **(D)** Annexin V staining and flow cytometric analyses were carried out to determine the impact of ST on the radioprotective effect of CAT in HSCs. **(E)** CFU assay was employed to examine the clonogenic function of HSPCs after different treatments. $^{a}P < 0.001$ versus CTL; $^{b}P < 0.05$ versus CTL; $^{c}P < 0.01$ versus IR + CAT.

enzyme; one molecule of CAT is capable of converting more than 6 million molecules of H_2O_2 to water and oxygen every minute. H_2O_2 is a major component of ROS and excessive accumulation of intracellular H_2O_2 can cause oxidative stress, resulting in apoptotic cell death. However, the effects of exogenous CAT treatment on IR-induced oxidative stress and apoptosis in HSPCs have not been reported until this study. Here, we demonstrate for the first time that exogenous CAT treatment can inhibit IR-induced DNA damage and apoptosis in HSPCs.

We and others have demonstrated that IR-induced ROS play a critical role in radiation tissue injury [10–12,18–20]. IR induces ROS production in irradiated cells as a consequence of radiolysis of water, which can cause DNA damage, ultimately leading to apoptosis and/or cellular senescence. The toxicity of ROS is modified by several antioxidant enzymes such as CAT, which function as ROS scavengers. In this study, we found that IR-induced apoptosis is associated with increased production of ROS in irradiated HSPCs. Moreover, the data showed that inhibition of ROS by CAT treatment attenuates IR-induced apoptosis and DNA damage in HSPCs. These results suggest that inhibition of IR-induced oxidative stress by exogenous CAT treatment could provide an effective strategy for protection of BM from radiation injury through inhibition of ROS production and ROS-mediated DNA damage in HSPCs.

It has been well documented that STAT3 is involved in modulating HSPC functions [26–29]. STAT3 also can provide cells with a survival advantage via promoting the expression of anti-apoptotic proteins such as BCL-2 and survivin [27,31]. Interestingly, we found here that the radioprotective effect of CAT is associated with increased STAT3 activation and elevated survivin expression, and that inhibition of STAT3 by ST abolishes the protective activity of CAT in HSPCs. These novel observations suggest that CAT may inhibit IR-induced oxidative stress, DNA damage, and apoptosis, at least in part, through activating the STAT3 signaling pathway. In support of this idea, it has been recently shown that STAT3 can bind to and affect the enzymatic activities of several subunit complexes of the mitochondrial electron-transport chain, thus demonstrating a new and noncanonical role for STAT3 in mitochondrial function [32,33]. Furthermore, in agreement with our findings, there is evidence that STAT3-deficient HSPCs show increased ROS levels and impaired self-renewal function [34]. Together, these results suggest that CAT may inhibit IR-induced oxidative stress and apoptosis in HSPCs via promoting STAT3 activation and, consequently, modulating mitochondrial function.

The mechanisms by which CAT activates STAT3 in HSPCs are unknown. However, it has been shown that H_2O_2 is involved in the regulation of several signaling pathways via modulating protein phosphorylation. In fact, H_2O_2 can modulate the activity of protein tyrosine phosphatases (PTPs) such as leukocyte antigen-related and PTP-1 [35]. Therefore, it is possible that CAT may regulate the phosphorylation and activation of STAT3 signaling in HSPCs through inhibition of H_2O_2 production, which, in turn, can modulate H_2O_2-mediated alterations in the functions of PTPs. Nevertheless, further in-depth mechanism studies are needed to better understand how CAT treatment activates the STAT3 signaling pathway in HSPCs.

In summary, this study demonstrates for the first time that exogenous CAT treatment protects murine HSPCs against radiation-induced DNA damage and apoptosis. We also have discovered a novel link between the radioprotective activity of CAT and activation of the STAT3 signaling pathway. These findings support further exploration of CAT as a radioprotective agent to ameliorate radiation-induced hematologic toxicity in vivo in a preclinical setting.

Acknowledgments

The authors want to thank Mrs. Aimin Yang for excellent technical assistance. This study was supported, in part, by a grant from the National Heart, Lung, and Blood Institute (NHLBI) no. HL106451 (G.Y.W.) and a pilot grant from the Hollings Cancer Center (G.Y.W.) via P30 CA138313.

Author Disclosure Statement

The authors declare no conflicts of interest.

References

1. Mauch P, L Constine, J Greenberger, W Knospe, J Sullivan, JL Liesveld and HJ Deeg. (1995). Hematopoietic stem cell compartment: acute and late effects of radiation therapy and chemotherapy. Int J Radiat Oncol Biol Phys 31:1319–1339.
2. Daniel D and J Crawford. (2006). Myelotoxicity from chemotherapy. Semin Oncol 33:74–85.
3. Meng A, Y Wang, SA Brown, G Van Zant and D Zhou. (2003). Ionizing radiation and busulfan inhibit murine bone marrow cell hematopoietic function via apoptosis dependent and independent mechanisms. Exp Hematol 31:1348–1356.
4. Johnso SM, M Torrice, JF Bell, KB Monahan, Q Jiang, Y Wang, MR Ramsey, J Jin, KK Wong, et al. (2010). Mitigation of hematologic radiation toxicity through pharmacological quiescence in mice. J Clin Invest 120:528–536.
5. Coleman CN, HB Stone, JE Moulder and TC Pellmar. (2004). Modulation of radiation injury. Science 304:693–694.
6. Wang Y, BA Schulte, AC Larue, M Ogawa and D Zhou. (2006). Total body irradiation selectively induces murine hematopoietic stem cell senescence. Blood 107:358–366.
7. Guinan EC, CM Barbon, LA Kalish, K Parmar, J Kutok, CJ Mancuso, L Stoler-Barak, EE Suter, JD Russell, et al. (2011). Bactericidal/permeability-increasing protein (rBPI21) and fluoroquinolone mitigate radiation-induced bone marrow aplasia and death. Sci Transl Med 3:110ra118.
8. Geiger H, SA Pawar, EJ Kerschen, KJ Nattamai, I Hernandez, HP Liang, JÁ Fernández, JA Cancelas, MA Ryan, et al. (2012). Pharmacological targeting of the thrombomodulin-activated protein C pathway mitigates radiation toxicity. Nat Med 18:1123–1129.
9. Hoggatt J, P Singh, KN Stilger, PA Plett, CH Sampson, HL Chua, CM Orschell and LM Pelus. (2013). Recovery from hematopoietic injury by modulating prostaglandin E(2) signaling post-irradiation. Blood Cells Mol Dis 50:147–153.
10. Wang Y, L Liu, S Pazhanisamy, A Meng and D Zhou. (2010). Total body irradiation selectively induces persistent oxidative stress in murine hematopoietic stem cells. Free Radic Biol and Med 48:348–356.
11. Shao L, H Li, SK Pazhanisamy, A Meng, Y Wang and D Zhou. (2011). Reactive oxygen species and hematopoietic stem cell senescence. Int J Hematol 94:24–32.
12. Li H, Y Wang, SK Pazhanisamy, L Shao, A Meng, I Batinic-Haberle and D Zhou. (2011). Mn(III) meso-tetrakis-(N-ethylpyridinium-2-yl) porphyrin mitigates total body irradiation-induced long-term bone marrow suppression. Free Radic Biol Med 51:30–37.
13. Datta K, S Suman, BV Kallakury and AJ Fornace, Jr. (2012). Exposure to heavy ion radiation induces persistent oxidative stress in mouse intestine. PLoS One 7:e42224.
14. Bucci B, S Misiti, A Cannizzaro, R Marchese, GH Raza, R Miceli, A Stigliano, D Amendola, O Monti, et al. (2006). Fractionated ionizing radiation exposure induces apoptosis through caspase-3 activation and reactive oxygen species generation. Anticancer Res 26:4549–4557.
15. Huang HL, LW Fang, SP Lu, CK Chou, TY Luh and MZ Lai. (2003). DNA-damaging reagents induce apoptosis through reactive oxygen species-dependent Fas aggregation. Oncogene 22:8168–8177.
16. Biaglow JE, JB Mitchell and K Held. (1992). The importance of peroxide and superoxide in the X-ray response. Int J Radiat Oncol Biol Phys 22:665–669.
17. Saada HN, UZ Said, NH Meky and AS Abd El Azime. (2009). Grape seed extract Vitis vinifera protects against radiation-induced oxidative damage and metabolic disorders in rats. Phytother Res 23:434–438.
18. Shao L, Y Luo and D Zhou. (2014). Hematopoietic stem cell injury induced by ionizing radiation. Antioxid Redox Signal 20:1447–1462.
19. Liao AC, BM Craver, BP Tseng, KK Tran, VK Parihar, MM Acharya and CL Limoli. (2013). Mitochondrial-targeted human catalase affords neuroprotection from proton irradiation. Radiat Res 180:1–6.
20. Shen H, H Yu, PH Liang, H Cheng, R XuFeng, Y Yuan, P Zhang, CA Smith and T Cheng. (2012). An acute negative bystander effect of γ-irradiated recipients on transplanted hematopoietic stem cells. Blood 119:3629–3637.
21. Miao W, R Xufeng, MR Park, H Gu, L Hu, JW Kang, S Ma, PH Liang, Y Li, et al. (2013). Hematopoietic stem cell regeneration enhanced by ectopic expression of ROS-detoxifying enzymes in transplant mice. Mol Ther 21:423–432.
22. Gupta R, S Karpatkin and RS Basch. (2006). Hematopoiesis and stem cell renewal in long-term bone marrow cultures containing catalase. Blood 107:1837–1846.
23. Wang Y, J Keller, L Liu and D Zhou. (2011). Inhibition of p38 mitogen-activated protein kinase promotes ex vivo hematopoietic stem cell expansion. Stem Cells Dev 20:1143–1152.
24. Luo H, A Yang, BA Schulte, MJ Wargovich and GY Wang. (2013). Resveratrol Induces Premature Senescence in Lung Cancer Cells via ROS-Mediated DNA Damage. PLoS One 8:e60065.
25. Luo H, L Wang, BA Schulte, A Yang, S Tang and GY Wang. (2013). Resveratrol enhances ionizing radiation-induced premature senescence in lung cancer cells. Int J Oncol 43:1999–2006.
26. Chung YJ, BB Park, YJ Kang, TM Kim, CJ Eaves and IH Oh. (2006). Unique effects of Stat3 on the early phase of hematopoietic stem cell regeneration. Blood 108:1208–1215.
27. Gu L, KY Chiang, N Zhu, HW Findley and M Zhou. (2007). Contribution of STAT3 to the activation of survivin by GM-CSF in CD34+ cell lines. Exp Hematol 35:957–966.

28. Hevehan DL, WM Miller and ET Papoutsakis. (2002). Differential expression and phosphorylation of distinct STAT3 proteins during granulocytic differentiation. Blood 99:1627–1637.
29. Oh IH and CJ Eaves. (2002). Overexpression of a dominant negative form of STAT3 selectively impairs hematopoietic stem cell activity. Oncogene 21:4778–4787.
30. Schust J, B Sperl, A Hollis, TU Mayer and T Berg. (2006). Stattic: a small-molecule inhibitor of STAT3 activation and dimerization. Chem Biol 13:1235–1242.
31. Lee JK, C Won, EH Yi, SH Seok, MH Kim, SJ Kim, MH Chung, HG Lee, K Ikuta and SK Ye. (2013). Signal transducer and activator of transcription 3 (Stat3) contributes to T-cell homeostasis by regulating pro-survival Bcl-2 family genes. Immunology 140:288–300.
32. Wegrzyn J, R Potla, YJ Chwae, NB Sepuri, Q Zhang, T Koeck, M Derecka, K Szczepanek, M Szelag, et al. (2009). Function of mitochondrial Stat3 in cellular respiration. Science 323:793–797.
33. Tammineni P, C Anugula, F Mohammed, M Anjaneyulu, AC Larner and NB Sepuri. (2013). The import of the transcription factor STAT3 into mitochondria depends on GRIM-19, a component of the electron transport chain. J Biol Chem 288:4723–4732.
34. Mantel C, S Messina-Graham, A Moh, S Cooper, G Hangoc, XY Fu and HE Broxmeyer. (2012). Mouse hematopoietic cell-targeted STAT3 deletion: stem/progenitor cell defects, mitochondrial dysfunction, ROS overproduction, and a rapid aging-like phenotype. Blood 120:2589–2599.
35. Denu JM and KG Tanner. (1998). Specific and reversible inactivation of protein tyrosine phosphatases by hydrogen peroxide: evidence for a sulfenic acid intermediate and implications for redox regulation. Biochemistry 37:5633–5642.

Address correspondence to:
Gavin Y. Wang, MD, PhD
Department of Pathology and Laboratory Medicine
Medical University of South Carolina
171 Ashley Avenue, MSC908
Charleston, SC 29425

E-mail: wangy@musc.edu

Received for publication August 13, 2014
Accepted after revision January 19, 2015
Prepublished on Liebert Instant Online January 20, 2015